Journal of Sensor Science and Technology
Vol. 33, No. 6 (2024) pp. 474-480
http://dx.doi.org/10.46670/JSST.2024.33.6.474
pISSN 1225-5475/eISSN 2093-7563

DPP-DTT Thin-Film-Transistor-based Glucose Sensor with Parylene C Gate Dielectric

Min-Joon Kim[1,*], Dong-Jun Han[1,*], Gwang-Eun Choi[1], Ra-Yeong Park[1], and Dong-Wook Park[1,+]

Abstract

Rapid and simple glucose detection is essential in healthcare, food safety, and environmental monitoring. This paper presents a flexible organic thin-film transistor glucose sensor using a PDPP2T-TT-OD (DPP-DTT) channel and Parylene C as both the substrate and gate dielectric. DPP-DTT is a high-mobility semiconductor material that enables simple and low-cost fabrication. Parylene C provides transparency, flexibility, and excellent chemical stability, thereby enhancing the durability of the sensor. The proposed glucose sensor was designed with a coplanar bottom-gate structure to enable direct contact between the DPP-DTT channel and the glucose solution. For the detection, the DPP-DTT channel was coated with glucose oxidase enzyme (GOx). Glucose solutions diluted in phosphate-buffered saline at the concentrations of 0 mM, 10 mM, and 25 mM were analyzed. The drift current that occurs during measurement and the time required for the sensor to rejuvenate are considered as limitations. Therefore, we performed calibration to improve the accuracy of the sensor. Consequently, the glucose sensors with the channel widths/lengths of 5000/50 (μm/μm) and 5000/75 (μm/μm) showed the sensitivities of 52.8946 nA/mM and 13.0305 nA/mM, respectively. This study highlighted the potential of a flexible and biocompatible glucose sensor using Parylene C and DPP-DTT. The proposed sensor is suitable for wearable health-monitoring applications.

Keywords: Glucose sensor, DPP-DTT, Parylene C, Microfluidic channel

1. INTRODUCTION

Electrical biosensing devices have contributed significantly to genomics, pharmacology, and clinical diagnostics [1,2]. These biosensors are characterized by their rapid response, high sensitivity, selectivity, and compact size. Various types of electrical biosensors have been developed, including electrochemical electrodes [3], field-effect transistors [4], surface acoustic wave sensors [5], and capacitors [6]. In this study, we developed a biosensor using an organic thin-film transistor (OTFT) for rapid glucose detection. OTFTs fabricated from organic materials are suitable for biosensing applications owing to their high flexibility and biocompatibility. PDPP2T-TT-OD (DPP-DTT) is an organic semiconductor material with high mobility and simplicity [7,8]. A recent study has investigated DPP-DTT in transistors, solar cells, and biosensors for detecting Interleukin-6 using antibodies [9]. In this study, Parylene C was utilized as the substrate and gate dielectric. Parylene C is well known for its transparency, flexibility, and excellent chemical stability, which considerably enhance the durability of the sensor [10]. By integrating a flexible, biocompatible Parylene C substrate and gate dielectric with a DPP-DTT-based OTFT, we developed a sensor with flexible and biocompatible properties [11]. Polymeric materials, such as poly(3,4-ethylenedioxythiophene)-poly(styrene sulfonate) (PEDOT:PSS), can switch between various redox states by changing their potential or pH [12,13]. A PEDOT:PSS-based glucose sensor demonstrated the reaction between glucose oxidase and glucose by measuring the change in the conductivity of a PEDOT:PSS gate electrode [14]. Another study developed a PEDOT:PSS OTFT biosensor by forming a PEDOT:PSS-GOx channel, which enabled direct enzymatic reactions with glucose solutions [15]. This study aimed to measure the change in the conductivity of the DPP-DTT channel resulting from the redox reactions of H_2O_2 produced by the interaction of glucose oxidase and glucose.

[1]School of Electrical and Computer Engineering, University of Seoul
Seoul 02504, Republic of Korea
*These authors are contrubuted equally to this work.
[+]Corresponding author: dwpark31@uos.ac.kr
(Received : Nov. 1, 2024, Revised : Nov. 7, 2024, Accepted : Nov. 13, 2024)

2. EXPERIMENTAL

2.1 Structure of DPP-DTT Glucose Sensor

The sensor was designed as a coplanar bottom-gate structure, enabling direct contact between the DPP-DTT channel and the glucose oxidase enzyme and glucose solution, as shown in Fig. 1 (a). Fig. 1 (b) and (c) show microscopic images of two types of OTFT channels fabricated on a silicon wafer, with the width-to-length ratios (W/L) of 5000/50 (μm/μm) and 5000/75 (μm/μm), respectively. Fig. 1 (d) illustrates the integration of a polydimethylsiloxane (PDMS) microfluidic channel with a DPP-DTT channel. If the glucose solution contacts the channel, source, and drain simultaneously, the ions in the solution can cause unwanted interference [16,17]. To prevent interference, the PDMS microfluidic channel was designed to be narrower than the OTFT channel, as shown in Fig. 1 (e). Furthermore, the proposed device can serve as a flexible and biocompatible biosensor by releasing the substrate material, Parylene C, as shown in Fig. 1 (f).

2.2 Fabrication of Glucose Sensor

A DPP-DTT glucose sensor was fabricated as shown in Fig. 2 (a).

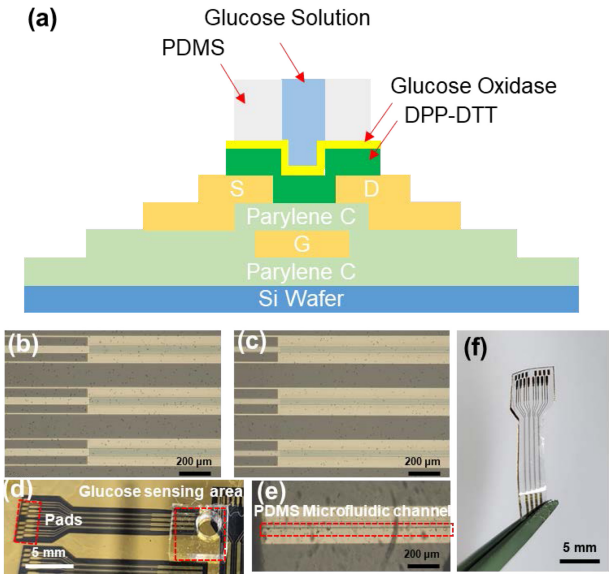

Fig. 1. Structure of the DPP-DTT glucose sensor. (a) Glucose sensor integrated with a PDMS microfluidic channel. Optical microscopy image of (b) channel of W/L = 5000/50 (μm/μm) and (c) channel of W/L = 5000/75 (μm/μm) transistor. (d) DPP-DTT glucose sensor aligned with the PDMS microfluidic channel. (e) Optical microscopy image of the aligned DPP-DTT and PDMS channels. (f) Flexible DPP-DTT glucose sensor released from Si wafer.

First, a 10-μm-thick Parylene C layer was deposited on a 4-inch silicon wafer via chemical vapor deposition to form the substrate. All the metal electrodes were made of titanium and gold (25/50 nm) and patterned using the liftoff method with an AZ5214E photoresist. After the deposition of the gate electrode, a 300-nm-thick Parylene C layer was deposited as the gate dielectric. The source and drain electrodes were patterned using the liftoff method with Ti/Au (25/50 nm). Subsequently, a solution of DPP-DTT dissolved in chloroform at 4 mg/mL for over 3 h was spin-coated at 1500 rpm for 30 s and then annealed at 150 °C for 10 min to form a DPP-DTT film of thickness approximately 550 nm [18]. Fig. 2 (b) shows the fabrication process of the PDMS microfluidic channel. The PDMS microfluidic channel was formed by applying a 10:1 mixture of SYLGARD 184 and a curing agent onto an SU-8-

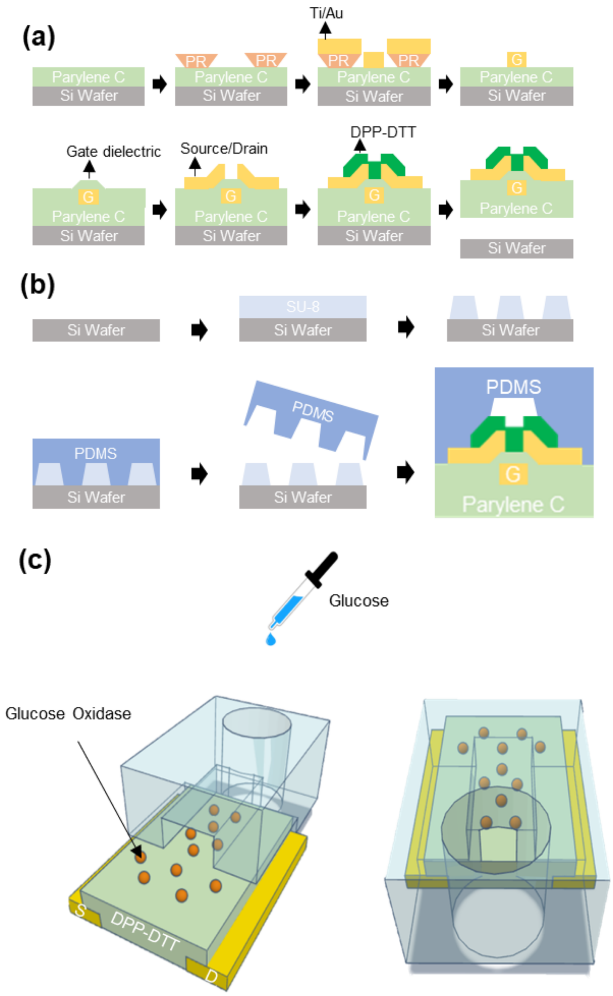

Fig. 2. Fabrication process of the glucose biosensor. (a) Fabrication process of the OTFT. (b) Fabrication process of the PDMS microfluidic channel. (c) Schematic of the 3D model showing the front and back sides of the DPP-DTT transistor channel functionalized with glucose oxidase, aligned with the PDMS microfluidic channel.

patterned silicon wafer. PDMS was then cured in a vacuum oven at 90 °C for 90 min. Finally, the PDMS microfluidic channel was peeled off, and the inlet was formed using a biopsy punch.

2.3 Surface Functionalization by Glucose Oxidase

GOx enzyme (10 mg, 250 KU) was diluted in 10 mL of a 1 × phosphate-buffered saline (PBS) solution and sprayed uniformly over the wafer using a spray gun. After approximately 3 h, the surface was rinsed with the 1× PBS solution and dried with nitrogen blowing before the electrical measurements. Subsequently, the DPP-DTT channel of the OTFT was aligned with the PDMS microfluidic channel under a microscope, and glucose solutions of varying concentrations were introduced through the inlet. Fig. 2 (c) shows a schematic of the 3D model of the experimental setup.

3. RESULTS AND DISCUSSIONS

3.1 Electrical Characteristics of DPP-DTT OTFT

Measurements of the transfer curves and the corresponding transconductance values are necessary to determine the optimal voltage range for sensor performance [19]. In Fig. 3 (a), the gate voltage was swept from −80 V to 40 V, with the drain voltage biased at −2 V, −10 V, and −30 V. Owing to the direct contact of the channel of the sensor with the solution during measurements, a low drain voltage of −2 V was chosen. Fig. 3 (b) shows the transconductance under the drain voltage bias of −2 V. The sensor shows a favorable transconductance up to a gate voltage of approximately −20 V. In this study, changes in the drain current were induced by the activity of the glucose oxidase enzyme applied to the DPP-DTT channel. Fig. 3 (c) illustrates this enzymatic reaction: in a glucose solution, α- and β-glucose exist in a ratio of approximately 36:64, where β-glucose reacts with glucose oxidase to produce gluconolactone and hydrogen peroxide. The DPP-DTT channel transitions to a redox state owing to hydrogen peroxide, resulting in changes in the drain current, a mechanism comparable to that observed for PEDOT:PSS [20].

3.2 Analysis of DPP-DTT Glucose Sensor

3.2.1 Detection of glucose

To validate the DPP-DTT glucose sensor, solutions containing 0 mM (1× PBS only), 10 mM, or 25 mM glucose (each diluted in 1× PBS) were injected into the inlet of the PDMS microfluidic

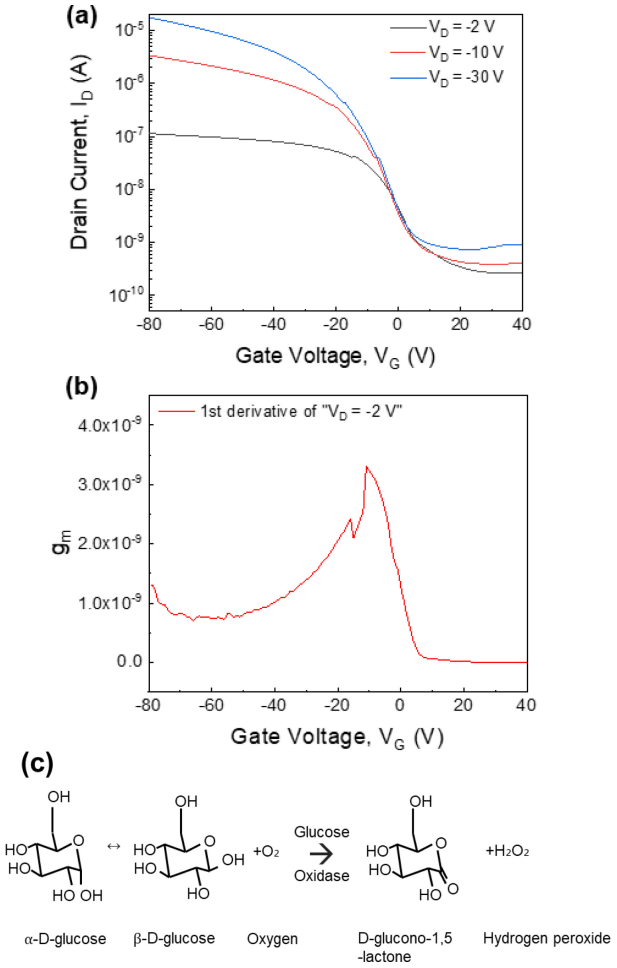

Fig. 3. Characteristics and mechanism of the DPP-DTT glucose biosensor. (a) Transfer curve of the DPP-DTT channel transistor. (b) Transconductance of the DPP-DTT channel transistor at V_D = −2 V. (c) Enzymatic reaction of the DPP-DTT glucose biosensor.

channel. Between each measurement for different glucose concentrations, the sensor was rinsed with 1× PBS, followed by a 5-min waiting period to allow the sensor to rejuvenate. The electrical characteristics of the sensor were measured using a probe station and Keithley 4200 semiconductor parameter analyzer, with the drain voltage biased at −2 V and the gate voltage swept from −5 V to 2 V to measure the drain current. Owing to the structure of the sensor, with the solution directly applied to the channel, the gate voltage was limited to −5 V to avoid degradation at higher voltages. To minimize errors in the initial measurement, the values were recorded starting from the fifth measurement of the operating voltage.

The drain current results for different channel W/L ratios are shown in Fig. 4 (a) and 4 (b). Similarly, to reduce the measurement errors, the drain currents at different glucose concentrations with a gate voltage of −4 V are shown in Fig. 4 (c) and 4 (d). For a

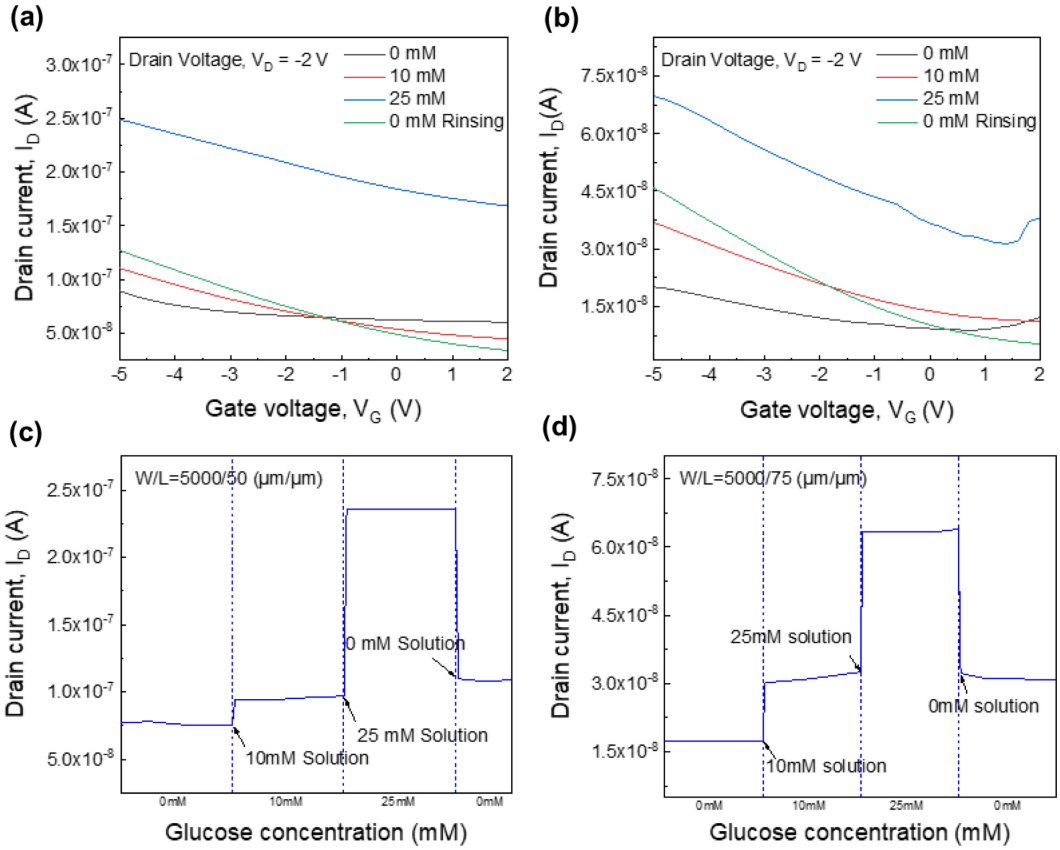

Fig. 4. (a) Transfer curve of the gate W/L = 5000/50 (μm/μm) transistor. (b) Transfer curve of the gate W/L = 5000/75 (μm/μm) transistor, (c) Drain current depending on the glucose concentration, at $V_G = -4$ V and $V_D = -2$ V, measured at different glucose concentrations with gate W/L = 5000/50 (μm/μm) and (d) gate W/L = 5000/75 (μm/μm).

channel W/L ratio of 5000/50 (μm/μm), the drain currents were measured as 76.3 nA, 95.2 nA, 236 nA, and 10.9 nA for 0 mM, 10 mM, 25 mM, and 0 mM (again) glucose solutions, to determine the difference from the initial value at the end. For a channel W/L ratio of 5000/75 (μm/μm), the corresponding drain currents were 17.4 nA, 31.3 nA, 63.5 nA, and 31.3 nA under the same conditions.

3.2.2 Calibration of detected drain current

After measuring a 25 mM glucose solution and subsequently rinsing to measure at 0 mM, the measured current did not return to its initial baseline, which was attributed to drift currents during the measurement process [21]. As glucose oxidase reacts with glucose, hydrogen peroxide is produced, generating H^+ ions. These H^+ ions then accumulate in traps between the gate dielectric (Parylene C) and the interface with the DPP-DTT channel, resulting in a continuous increase in the drain current.

Data calibration was applied to ensure that the drain currents for the initial and final 0 mM glucose measurements were equivalent. This calibration assumed that the generated hydrogen peroxide increased proportionally with the glucose concentration and that the number of traps in the gate dielectric and between the dielectric and the channel also increased proportionally. Upon returning to 0 mM, the ions generated from prior glucose measurements were assumed to have a sustained effect proportional to the glucose concentration. Therefore, the glucose concentration was considered constant, and a proportional weighting factor was applied to correct for drift based on the glucose concentration. The results before and after correction are listed in Table 1.

Table 1. Analysis of drain current before and after calibration

Drain Current (nA)			
Before calibration		After calibration	
5000/50 (μm/μm)	5000/75 (μm/μm)	5000/50 (μm/μm)	5000/75 (μm/μm)
76.3	17.4	76.3	17.4
95.2	31.3	85.9	27.3
236	63.5	203	49.6

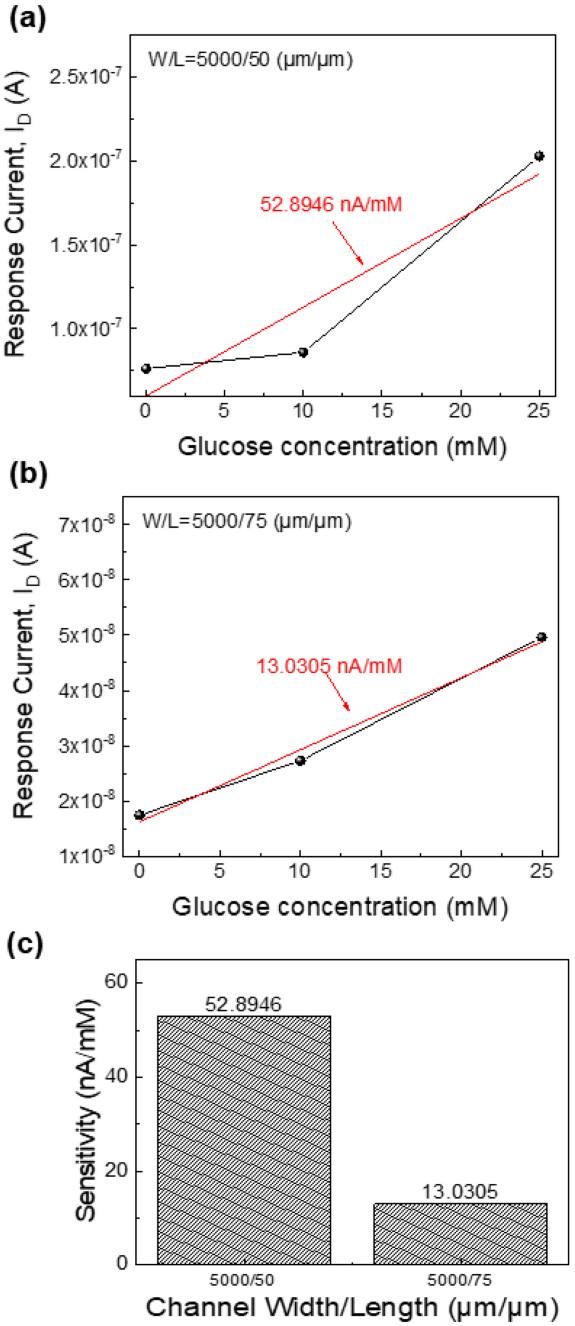

Fig. 5. Calibrated data of the drain current depending on the glucose concentration, at $V_G = -4$ V and $V_D = -2$ V with (a) channel W/L = 5000/50 (μm/μm) and (b) gate W/L = 5000/75 (μm/μm). The red line is the linear fit of the displayed data points. (c) Sensitivity of two different channel sizes.

3.3 Sensitivity Variation According to Channel Length

The DPP-DTT OTFTs have a channel width of 5000 μm and two different channel lengths, 50 μm and 75 μm. A DPP-DTT OTFT with a shorter channel length and higher transconductance is expected to exhibit greater sensitivity [22]. Fig. 5 (a) and 5 (b) illustrate the drain currents for various glucose concentrations with a linear fit, showing a sharp sensitivity increase for the 5000/50 (μm/μm) sensor at 25 mM. The sensitivity calculated using a linear fit is shown in Fig. 5 (c).

$$\text{Sensitivity (aA/mM)} = \frac{\Delta I_D}{\Delta mM} \quad (1)$$

For the DPP-DTT glucose sensor with the channel W/L of 5000/50 (μm/μm), a sensitivity of 52.8946 nA/mM was observed, whereas the DPP-DTT glucose sensor with the channel W/L of 5000/75 (μm/μm) showed a sensitivity of 13.0305 nA/mM. Overall, it was confirmed that the shorter sensors exhibited higher sensitivity.

4. CONCLUSIONS

In this study, an OTFT-based glucose sensor was developed by integrating Parylene C and DPP-DTT into a PDMS microfluidic channel. The drain current changes in the DPP-DTT glucose sensor were monitored at various glucose concentrations, and the drift current was calibrated. It is challenging to fabricate a sensor that operates without drifting [23].

The basic idea of drift compensation algorithms is to eliminate the variations in the sensor signal ascribed to sensor drift. This paper proposed a simple one-point calibration method. Various methods for calibrating sensor data have been suggested, with ongoing studies focusing on circuit-based correction techniques [24] and algorithmic approaches [25].

The rejuvenation of biosensors is also a critical factor in ensuring their durability and suitability for repeated use. While functionalization after each use is one approach, alternative methods, such as chemical treatment, the application of electric fields, and controlled heating, are being explored to enhance sensor longevity. Further studies are required to optimize the biosensor rejuvenation [26].

In this study, under a fixed width of 5000 μm, the DPP-DTT glucose sensor showed the sensitivities of 52.8946 nA/mM for a length of 50 μm and 13.0305 nA/mM for a length of 75 μm, highlighting sensitivity differences based on the channel length. Future studies could further enhance sensitivity by optimizing the W/L ratio. The flexibility and biocompatibility of the sensor suggest its potential for wearable skin-adherent applications.

ACKNOWLEDGMENT

This study was supported by the Ministry of Science and ICT

(MSIT), Korea, under the Information Technology Research Center (ITRC) support program (IITP-2024-RS-2023-00260091) supervised by the Institute for Information & Communications Technology Planning & Evaluation (IITP), and the National R&D Program through the National Research Foundation of Korea (NRF) funded by the MSIT (grant no. No. RS-2024-00411764, 2021M3H2A1038042). It was also partly supported by a Korea Institute for Advancement of Technology (KIAT) grant funded by the Korean Government (MOTIE) (P0017011, HRD Program for Industrial Innovation). The EDA Tool was supported by the IC Design Education Center.

REFERENCES

[1] C. Wang, W. Ye, Y. Li, Y. Zhu, Q. Lin, and M. He, "Exploiting electrostatic shielding-effect of metal nanoparticles to recognize uncharged small molecule affinity with label-free graphene electronic biosensor", *Biosens. Bioelectron.*, Vol. 129, pp. 93-99, 2019.

[2] M. R. Leyden, R. J. Messinger, C. Schuman, T. Sharf, V. T. Remcho, T. M. Squires, and E. D. Minot, "Increasing the detection speed of an all-electronic real-time biosensor", *Lab. Chip*, Vol. 12, No. 5, pp. 954-959, 2012.

[3] D. Sun, Z. Luo, J. Lu, S. Zhang, T. Che, Z. Chen, and L. Zhang, "Electrochemical dual-aptamer-based biosensor for nonenzymatic detection of cardiac troponin I by nanohybrid electrocatalysts labeling combined with DNA nanotetrahedron structure", *Biosens. Bioelectron.*, Vol. 134, pp. 49-56, 2019.

[4] H. Xie, Y. T. Li, Y. M. Lei, Y. L. Liu, M. M. Xiao, C. Gao, D. W. Pang, W. H. Huang, Z. Y. Zhang, and G. J. Zhang, "Real-time monitoring of nitric oxide at single-cell level with porphyrin-functionalized graphene field-effect transistor biosensor", *Anal. Chem.*, Vol. 88, No. 22, pp. 11115-11122, 2016.

[5] J. Andrä, A. Böhling, T. M. A. Gronewold, U. Schlecht, M. Perpeet, and T. Gutsmann, "Surface acoustic wave biosensor as a tool to study the interaction of antimicrobial peptides with phospholipid and lipopolysaccharide model membranes", *Langmuir*, Vol. 24, No. 16, pp. 9148-9153, 2008.

[6] S. Niyomdecha, W. Limbut, A. Numnuam, P. Kanatharana, R. Charlermroj, N. Karoonuthaisiri, and P. Thavarungkul, "Phage-based capacitive biosensor for Salmonella detection", *Talanta*, Vol. 188, pp. 658-664, 2018.

[7] Y. Li, S. P. Singh, and P. Sonar, "A high mobility P-type DPP-thieno 3,2-b thio-phene copolymer for organic thin-film transistors," *Adv. Mater.*, Vol. 22, No. 43, pp. 4862-4866, 2010.

[8] Y. Zhang, X. Yao, and Y. Cui, "A DPP-DTT Field-Effect Transistor-Based Biosensor for Detecting Interleukin-6", *IEEE Sens. Lett.*, Vol. 7, No. 1, pp. 1-4, 2022.

[9] J. Li, Y. Zhao, H. S. Tan, Y. Guo, C. A. Di, G. Yu, Y. Liu, M. Lin, S. H. Lim, Y. Zhou, H. Su, and B. S. Ong, "A stable solution-processed polymer semiconductor with record high- mobility for printed transistors", *Sci. Rep.*, Vol. 2, p. 754, 2012.

[10] H. Kwon, H. Ye, T. K. An, J. Hong, C. E. Park, Y. Choi, S. Shin, J. Lee, S. H. Kim, and X. Li, "Highly stable flexible organic field-effect transistors with Parylene-C gate dielectrics on a flexible substrate", *Org. Electron.*, Vol. 75, p. 105391, 2019.

[11] K. M. Kim, S. Kim, A. H. Hong, Y. Ko, H. Jang, H. Kim, and D. W. Park, "Development of Organic Thin-film Transistors on a Biocompatible Parylene-C Substrate", *J. Semicond. Technol. Sci.*, Vol. 23, No. 1, pp. 1-7, 2023.

[12] M. Chen, "Printed electrochemical devices using conducting polymers as active materials on flexible substrates", *Proc. IEEE*, Vol. 93, No. 7, pp. 1339-1347, 2005.

[13] A. Ernst, O. Makowski, B. Kowalewska, K. Miecznikowski, and P. J. Kulesza, "Hybrid bioelectrocatalyst for hydrogen peroxide reduction: immobilization of enzyme within organic–inorganic film of structured Prussian Blue and PEDOT", *Bioelectrochemistry*, Vol. 7, No. 1, pp. 23-28, 2007.

[14] D. J. Macaya, M. Nikolou, S. Takamatsu, J. T. Mabeck, R. M. Owensb, and G. G. Malliaras, "Simple glucose sensors with micromolar sensitivity based on organic electro-chemical transistors", *Sens. Actuators B Chem.*, Vol. 123, pp. 374-378, 2007.

[15] J. Liu, M. Agarwal, and K. Varahramyan, "Glucose sensor based on organic thin film transistor using glucose oxidase and conducting polymer", *Sens. Actuators B Chem.*, Vol. 135, pp. 195-199, 2008.

[16] S. Li, Y. Duan, W. Zhu, S. Cheng, and W. Hu, "Sensing Interfaces Engineering for Organic Thin Film Transistors-Based Biosensors: Opportunities and Challenges", *Adv. Mater.*, p. 2412379, 2024.

[17] T. Cramer, A. Campana, F. Leonardi, S. Casalini, A. Kyndiah, M. Murgia, and F. Biscarini, "Water-gated organic field effect transistors–opportunities for biochemical sensing and extracellular signal transduction", *J. Mater. Chem. B*, Vol. 1, No. 31, p. 3728, 2013.

[18] Y. Ko, H. W. Jang, H. Kim, and D. W. Park, "Analysis of electrical and hysteresis characteristics of flexible OTFT using solution-processable DPP-DTT polymer and Parylene-C", *Solid-State Electronics*, Vol. 216, p. 108922, 2024.

[19] P. Dwivedi and A. Kranti, "Applicability of transconductance-to-current ratio (gm/Ids) as a sensing metric for tunnel FET biosensors", *IEEE Sens. J.*, Vol. 17, No. 4, pp. 1030-1036, 2017.

[20] V. Syritski, K. Idla, and A. Öpik, "Synthesis and redox behavior of PEDOT/PSS and PPy/DBS structures", *Synth. Met.*, Vol. 144, No. 3, pp.235-239, 2004.

[21] G. E. Choi, M. J. Kim, R. Y. Park, Y. Kim, and D. W. Park, "InGaZnO Thin-Film Transistor-based pH Sensor with Parylene-C Gate Dielectric", *J. Sens. Sci. Technol.*, Vol. 33, No. 5, pp. 338-343, 2024.

[22] S. Demuru, J. Kim, M. El Chazli, S. Bruce, M. Dupertuis, P. A. Binz, M. Saubade, C. Lafaye, and D. Briand, "Antibody-coated wearable organic electrochemical transistors for cortisol detection in human sweat", *ACS Sens.*, Vol. 7,

No. 9, pp. 2721-2731, 2022.
[23] J. E. Haugen, O. Tomic, and K. Kvaal, "A calibration method for handling the temporal drift of solid state gas-sensors", *Anal. Chim. Acta*, Vol. 407, No. 1-2, pp. 23-39, 2000.
[24] P. Y. Kuo and Z. X. Dong, "A new calibration circuit design to reduce drift effect of RuO2 urea biosensors", *Sensors*, Vol. 19, No. 20, p. 4558, 2019.
[25] X. Jin, A. Cai, T. Xu, and X. Zhang, "Artificial intelligence biosensors for continuous glucose monitoring", *Interdiscip. Mater.*, Vol. 2, No. 2, pp. 290-307, 2023.
[26] Y. Jia, S. Chen, Q. Wang, and J. Li, "Recent progress in biosensor regeneration techniques", *Nanoscale,* Vol. 16, No. 6, pp. 2834-2846, 2024.